Advanced Optical Techniques for Measurements of Atmospheric Constituents

David M. Brown, Adam Willitsford, Kebin Shi, Zhiwen Liu, and C. Russell Philbrick
The Pennsylvania State University
Department of Electrical Engineering
University Park, PA 16802

Abstract - Spectral models available for calculations of optical propagation conditions provide the research and development community valuable tools for design, simulation, and validation of remote sensing techniques. Examples of these techniques applied to lidar developments are described. A white light super continuum laser has been proposed as a new tool for measurements of minor species concentrations on long paths in the atmosphere. The result from a recent experiment demonstrates the potential for Differential Absorption Spectroscopy (DAS) measurements. A controlled water vapor absorption path has been measured in the laboratory using a white light laser. Absorption measurements are compared with simulations from MODTRAN™ 4 and 5 to examine the water vapor band between 1300 and 1500 nm. Measurements of various atmospheric constituents can be accomplished by utilizing spectral features in the MWIR and LWIR fingerprint regions. Examination of the PNNL infrared spectral database in conjunction with MODTRAN™ 5 model calculations are used to show the feasibility of this technique. The study includes simulation of the broadband infrared detection techniques for mid-wave and long-wave IR regions with varied atmospheric conditions.

I. INTRODUCTION

Aside from the various government and commercial uses of spectral models like MODTRAN™, the research and development community additionally benefits from the completeness and attention to detail realized when building such a model. Models of this caliber are the frontrunners in the research and development process, as they allow for adaptation and modifications to achieve the goal at hand.

Recent research within the Department of Electrical Engineering at Penn State University has had the benefit of utilizing the MODTRAN™ 5 spectral model to validate experimental results of various research projects. Perhaps one of the most promising areas of study currently utilizing the MODTRAN™ 5 spectral model is the field of supercontinuum white light remote sensing. While the supercontinuum [Alfano, 1989] white light laser has been utilized in the research and development community for many years, only recently have we begun to use it for remote sensing applications. The Ultrafast Optics Laboratory within the Department of Electrical Engineering at Penn State studies the application of supercontiuum white light, and has worked with the researchers at the Penn State University Lidar Laboratory in an attempt to further develop this field.

II. SUPERCONTINUUM WHITE LIGHT LASER FOR WATER VAPOR MEASUREMENTS

The launching of short (e.g., femtosecond) laser pulses into a highly nonlinear photonic crystal fiber creates very broadband laser light [Ranka et al., 2000 and Knight et al., 1996]. For instance, supercontinuum white light can be generated by coupling sub-nanosecond laser pulses from a passively Q-switched microchip laser (JDSU NP-10620-100, wavelength at 1064 nm, average power ~ 40 mW) into a photonic crystal fiber (Blaze Photonics SC-5.0-1040). A typical spectrum, beginning at 500 nm and extending out into the near infrared beyond 1600 nm, measured by an Ando (now Yokogawa) optical spectrum analyzer (AQ6315E), is shown in Figure 1.

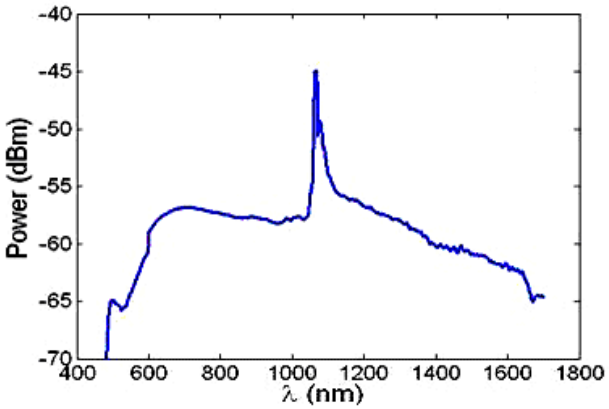

Figure 1. A typical spectrum of the supercontinuum white light generated by coupling subnanosecond laser pulses into a photonic crystal fiber

The ultra high spatial coherence and low temporal coherence (i.e., large bandwidth) of the supercontinuum white light make it possible to generate a nearly perfect temporally incoherent point light source as shown by Figure 2. It is the broad bandwidth and high spatial coherence characteristics that are particularly useful for remote sensing applications.

An experiment was performed utilizing the supercontinuum white light laser to measure atmospheric water vapor content along a folded path. The simple experimental setup shown in Figure 3 describes the arrangement of mirrors used to allow the laser to traverse a 20 m path and then be coupled into the optical spectrometer.

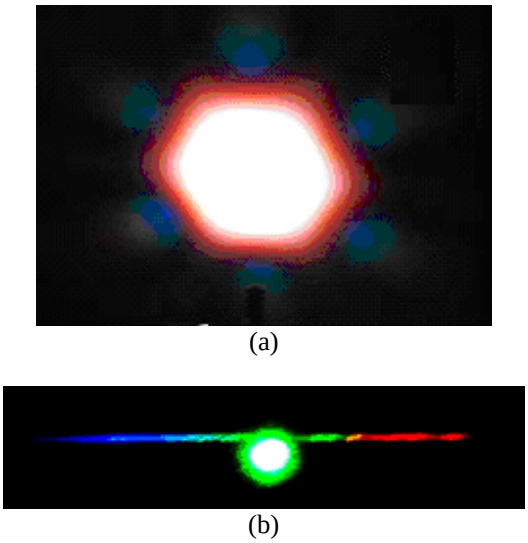

Figure 2. (a) The far field pattern of the supercontinuum white light generated by coupling femtosecond laser pulses into a photonic crystal fiber. (b) A rainbow observed after the collimated white light passes through a prism.

To select the wavelength location for examination using the Ando spectrum analyzer, we calculated the horizontal transmission for a 20 m path using the MODTRAN™ 4 model. We selected the water vapor absorption band in the near infrared region between 1300 and 1500 nm (~7700 and 6700 cm^{-1}). The data measured with the spectrometer near the wings of the band, 1300-1340 nm and 1420-1500 nm, are shown in Figure 5, along with an additional estimate of the instrument function superimposed on the experimental data.

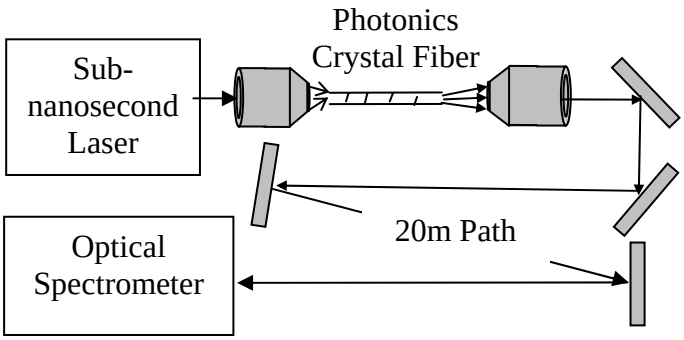

Figure 3. Experimental setup used to experimentally measure water vapor spectrum with supercontinuum white light.

Outside of the band of strong water vapor absorption, the experimental data was compared to the power spectrum of the white light laser. The poor correlation suggests that the instrument function is influenced by the various mirrors used to fold 20 m path, the optics used couple the output into the optical spectrometer, and the detector performance. Ideally, this response can be removed to determine a base line experiment.

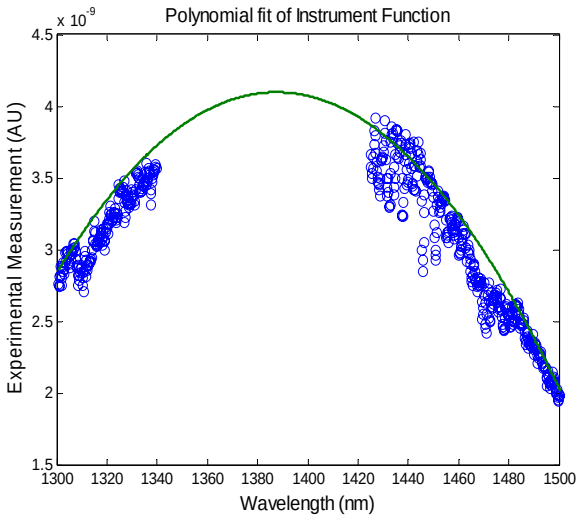

Figure 4. Normalization of experimental data utilizing polynomial fitting of non-absorbing wavelength ranges.

An alternate way of removing the instrument function from the experimental data set was used to provide an absorption profile that could then be accurately compared to MODTRAN simulation results. By fitting an approximate instrument function to the experimental data outside of the water vapor absorption band we are able to normalize the experimental data without the need of a base line measurement. The result of a comparison when the spectrum analyzer resolution is set to match the 1 cm^{-1} resolution of MODTRAN™ 4 is shown in Figure 6. After examining the wavelength band of water vapor absorption, the 40 nm band of wavelengths between 1380 and 1420 nm was selected for an additional higher resolution data collection and subsequent comparison. Prior to the acquisition of MODTRAN™ 5, the interpretation of this dataset was limited by the 1 cm^{-1} resolution of the MODTRAN™ 4 model, which did not possess the sufficient resolution to make an appropriate comparison. With the increased resolution of MODTRAN™ 5 update, the higher resolution data could be accurately represented, and is shown in Figure 7 for the wavelength band of interest. Figures 7 and 8 show comparisons when the resolution of the MODTRAN™ 5 simulation was adjusted to match the 0.4 cm^{-1} resolution of the Ando spectrum analyzer. Figure 8 highlights the excellent agreement in the 1400 to 1420 nm range. The plot includes the result for the 0.1 cm^{-1} simulation which shows the full capability of the MODTRAN™ 5 model and provides additional comparison. The techniques demonstrated with the example of water vapor detection shown can be extended to characterize additional atmospheric constituents of low concentrations by using increased path lengths, longer integration times, higher laser power, and improved spectrometer sensitivity and collection efficiency. The analysis of the spectral data leads the determination of a value of 37% relative humidity along the 20 m path, and this agrees well with the measured value from a sling psychrometer recorded at the time (Begnoché, 2005).

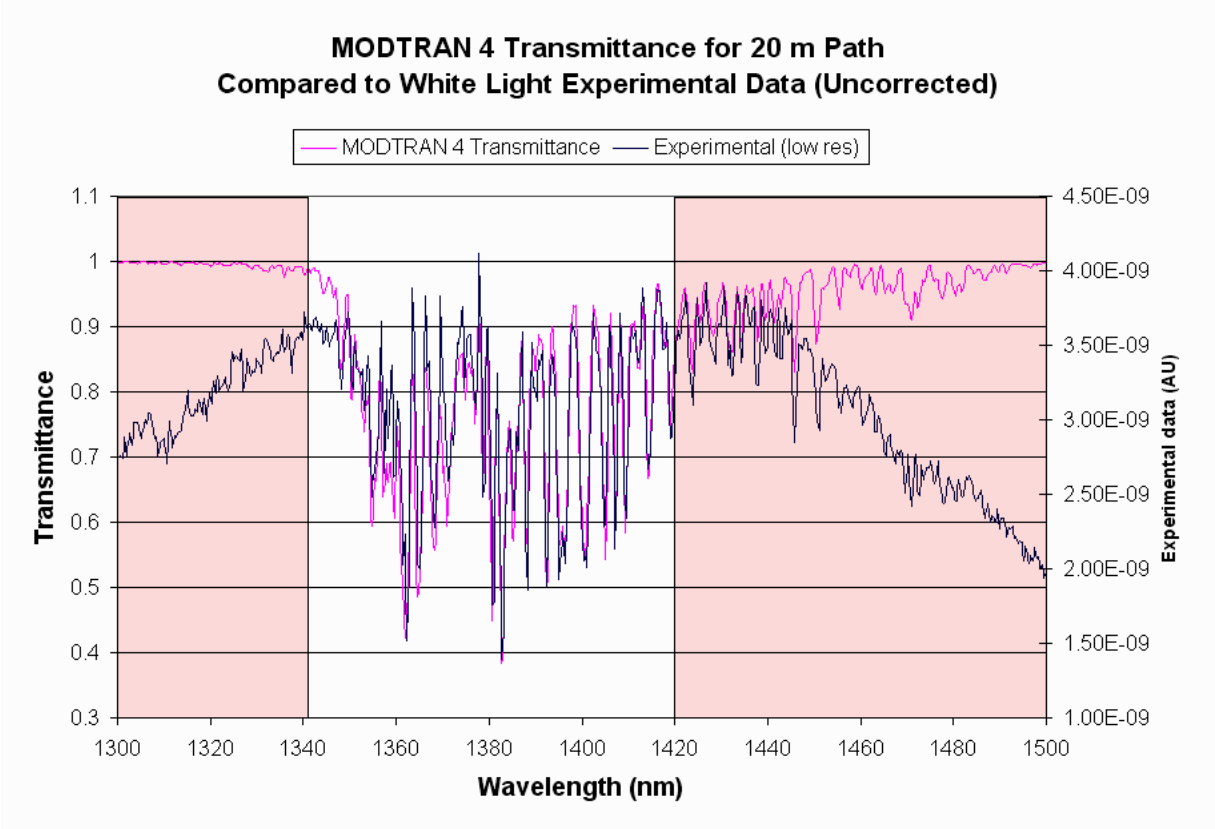

Figure 5. Water vapor transmittance 1300 -1500 nm experimental (blue) compared to MODTRAN™4 (pink).

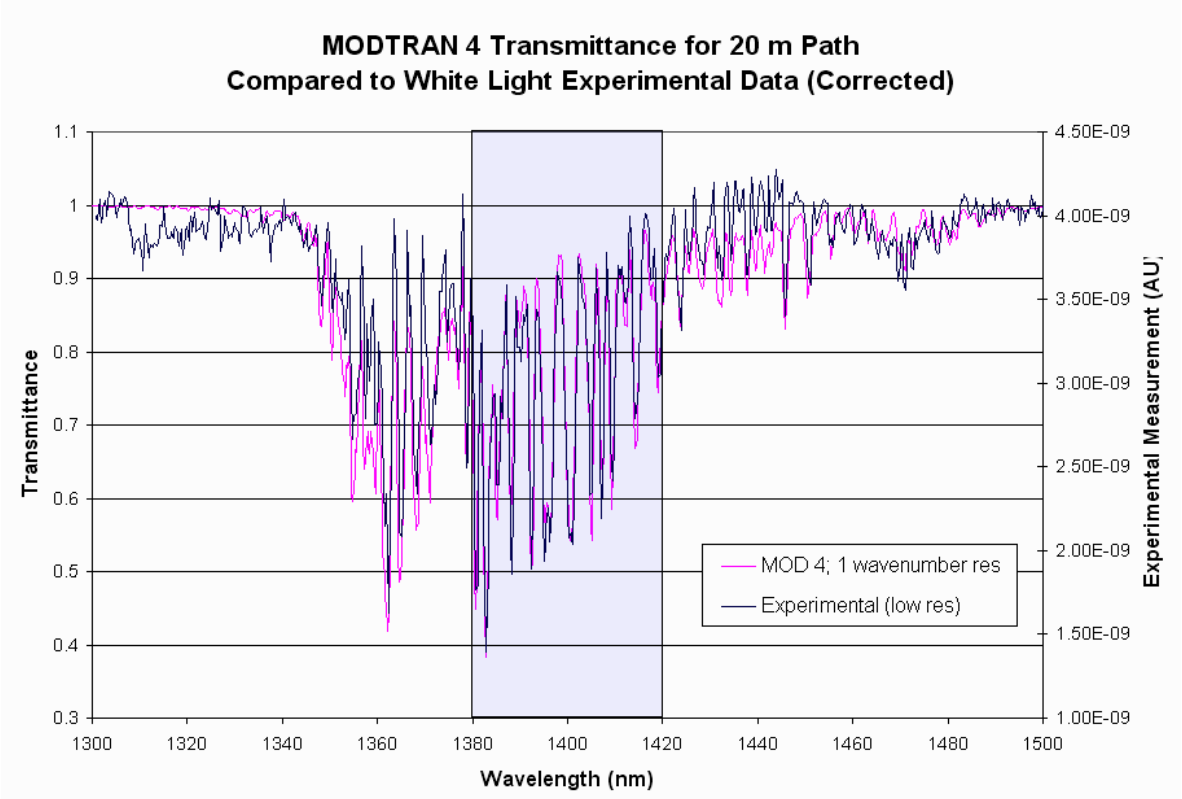

Figure 6. Water vapor transmittance 1300 -1500 nm experimental (blue) compared to MODTRAN™4 (pink), with the instrument function removed.

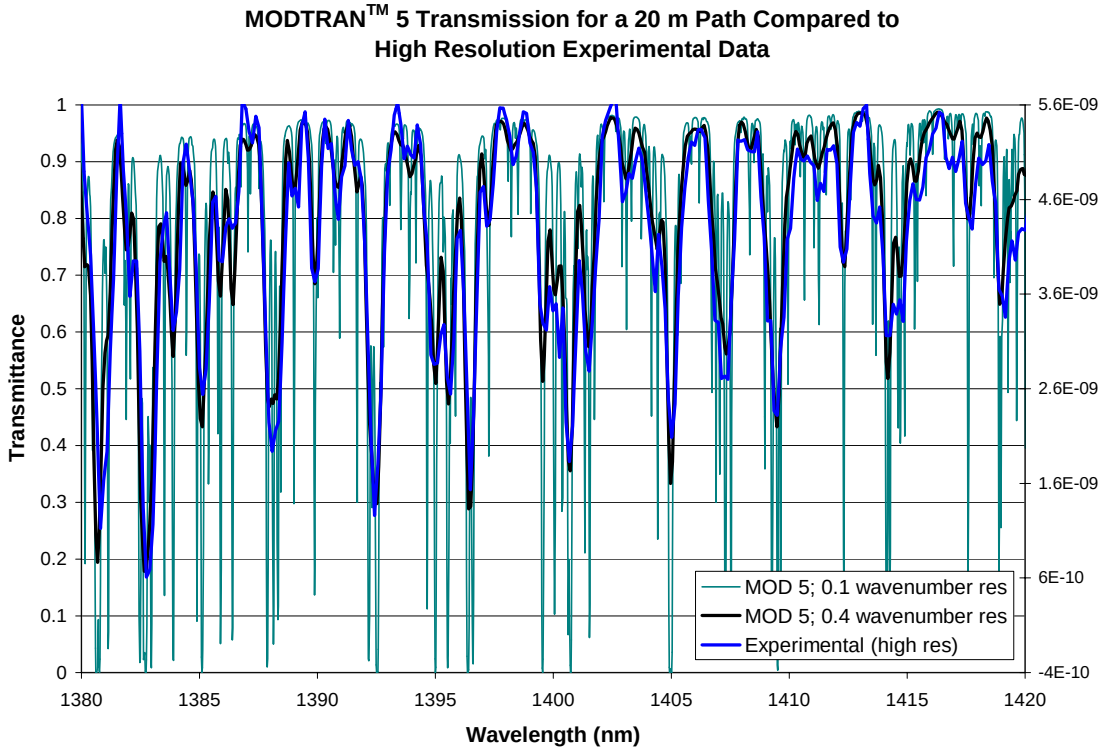

Figure 7. Water vapor transmittance 1380 - 1420 nm MODTRAN™5 compared to experimental.

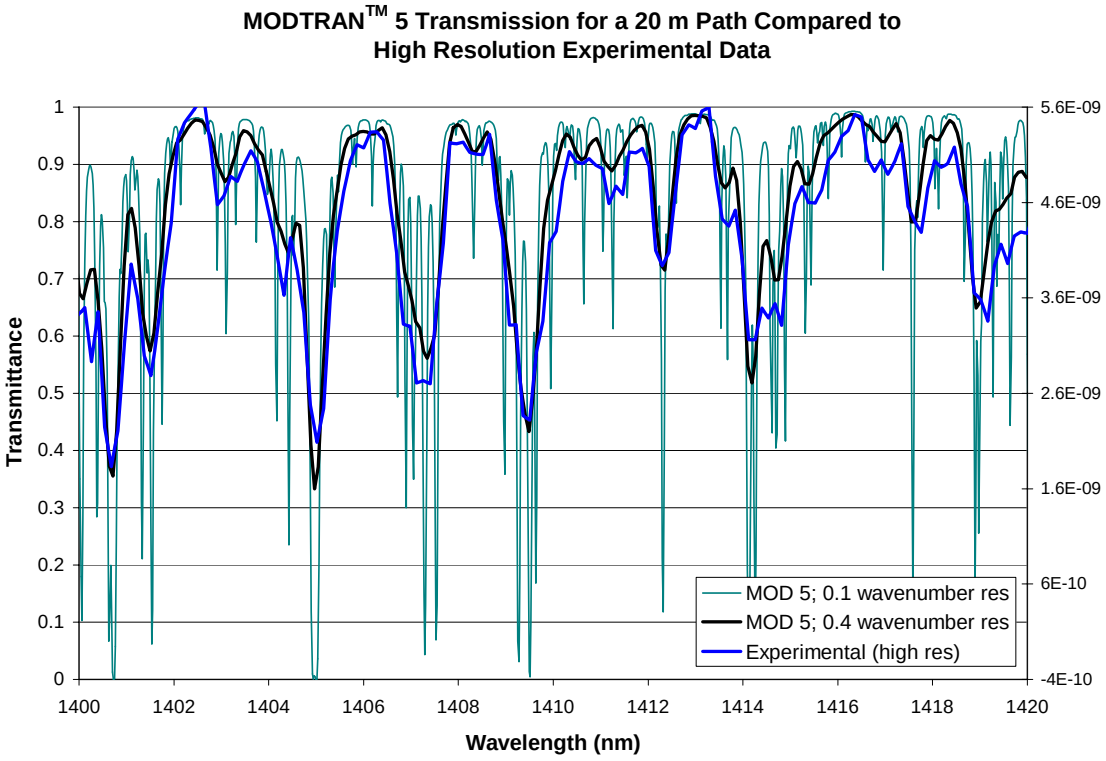

Figure 8. Water vapor transmittance 1400 - 1420 nm MODTRAN™5 compared to experimental.

III. MEASUREMENTS OF TRACE CONSITUTENTS

The MODTRAN™ 5 update has also provided a mechanism to simulate broadband absorption by a spatially distributed target. The method for remote sensing of absorption, such as that typically used in DAS (Differential Absorption Spectroscopy) remote sensing, often uses a passive source, namely the surface of the earth. Utilizing the MODTRAN™ 5 transmission code, we are able to simulate the broadband absorption effect of atmospheric constituent concentrations. With proper filtering, this absorption is detectable with current commercially available hardware. By utilizing the PNNL Infrared Spectral Database, we are able to design instruments that will yield the most significant absorption effects, and consequently best performance.

This method of remote detection is able to answer various environmental monitoring concerns. To demonstrate this capability, we initially examine nitrous oxide spectra as an example target. In addition to the strong greenhouse effects of nitrous oxide emissions, the accurate monitoring of N_2O emissions from motor vehicles has recently been the topic of debate. As outlined by [Lipman, 2002] many variables directly affect the amount of N_20 emitted by internal combustion engines, ranging from driving cycle, to catalytic converter type, and combustion dynamics. Additionally, it is interesting to note that mechanisms driving increased N_2O emissions from automobiles are not the combustion process, but instead emission control system. With diverse emission control mechanisms across all categories of automobile manufactures, it is easy to conclude that the range of N_2O emission will vary [Lipman, 2002]. On the average for late model vehicles, N_2O emissions appeared to be on the order of 5 ppm (parts per million) with a standard deviation of nearly 24 ppm. Earlier publications suggested that N_2O exhaust concentrations could exceed 400 ppm with certain emission control hardware. With such a large variation in estimated emission range of N_2O, we have chosen to explore possible detection and quantification methods. In addition, we have chosen to explore the detection possibilities for carbon monoxide (CO) with similar techniques. While CO detectors are quite common, with proper filtering, the following method of detection would provide observations of carbon monoxide plumes. This would be particularly useful when attempting to track and map the permeation of the compound for various applications. With CO concentrations of 5000 ppm being quickly fatal, concerns can be quickly realized when reviewing nominal concentrations of 30,000 ppm for undiluted cigarette smoke, 7,000 ppm for warm car exhaust about, and 5,000 ppm for chimney of a home wood fire. [Gosink, 1983] The reported detection methodology that follows was performed for cases of increased ground level plumes of CO and N_2O.

To begin, we have simulated a case of downlooking radiance from an altitude of 150 m for the midwave infrared under typical atmospheric conditions with the 1976 US Standard Atmosphere Model. The radiance calculated for this case is shown in Figure 9 as the solid blue line denoted as atmospheric N_2O. Based on a background concentration of 0.5 ppm of N_2O, the atmospheric path spectrum is dominated in this region by the N_2O signature. This structure in the vicinity of 3.85 to 3.95 µm, and again from 4.0 to 4.1 µm, is a result of atmospheric N_2O absorbing energy from the thermal background corresponding to specific vibrational states. These effects are intensified when the concentration of the N_2O is increased. The red line on the same plot corresponds to an increased concentration of N_2O at ground level to simulate what might be observed under the case of a heavily polluting automobile. The 50 ppm·m plume of N_2O was created in MODTRAN™ 5 by utilizing the user specified option to modify the atmospheric surface layers in the model. In order to simulate precisely 50 ppm·m, a single layer 1 meter in depth above the surface was specified to have a nitrous oxide concentration of 50 ppm by volume. As is apparent from the plot, the increased N_2O generates a significant modification in the observed radiant emittance as a function of wavelength.

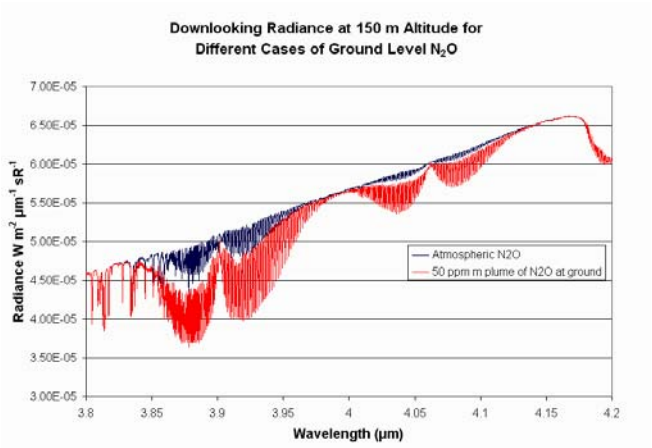

Figure 9. Downlooking radiance at 150 m altitude for N_2O, atmospheric N_2O is in blue and 50 ppm·m plume is shown in red.

Using the MODTRAN 5 simulations of various plumes of N_2O and CO, we have implemented an algorithm to calculate the total available radiance in a given wavelength range. Utilizing the highest resolution MODTRAN™5 radiance data (0.1 cm^{-1}) and analysis programs developed at Penn State, we have been able to characterize the captured radiance for a user specified wavelength range as shown in Figure 10. The Penn State algorithm uses the MODTRAN™ 5 simulation output to integrate the area bounded by the radiance curve for a specified wavelength range. The result is a single value of total radiant emittance "seen" at the given altitude of observation. Physically, the measurement represents the radiance captured by a broadband detector fitted with a filter corresponding to the wavelength parameters selected by the user.

While this analysis tool supports a variety of designs for filter transmission specification, the CO detection example shown in Figure 10 utilizes a rectangular filter with 95% transmission between 4.5 and 4.7 µm and 100% rejection

outside. By means of the MODTRAN™ 5 model, the integrated radiance emittance is calculated to be 0.83 Wm^{-2}, corresponding to an average surface temperature of 17 °C. Note the steradian dependence has been removed from the radiance information. Cancellation of the steradian dependence from the radiance information (and consequently from the total integrated radiant emittance) is justified by assuming the device used for measurement at the observation altitude has a fully filled field of view while configured in the downlooking orientation. When the CO concentration at ground level is increased to 600 ppm·m the signature between 4.5 and 4.7 μm is intensified, and is shown by Figure 11. The increased percentage of absorption is approximately 15% of the total integrated radiant emittance observed when simulated under nominal atmospheric concentrations of CO. To capitalize on this absorption effect, we must examine the following two factors that will determine the feasibility for using passive detection,

1. detector detection limit (sensor threshold), and
2. detector sensitivity limit (contrast).

For example, in order to clearly detect increased concentrations of CO at ground level, the detector detection limit must lie beneath 0.83 Wm^{-2}. With similar constraints, the sensitivity limit of the detector must be above the difference in radiant emittance for the plume present to the plume absent cases, namely greater than 0.12 Wm^{-2}. These numbers although specific for CO via the reviewed example, are outputs from the analysis using the MODTRAN™ 5 simulation. Therefore, trivial modifications to the MODTRAN™ 5 input file allows similar processing options for any MODTRAN™ 5 supported species.

Broadband absorption and scattering creates sufficient variation in observed downlooking radiance from a given altitude to detect the concentration of many interesting species. What hardware would be used to capitalize on such a slight variation in an effective manner? With both of these examples utilizing the midwave infrared (MWIR), we consider hardware possibilities supporting this region of the spectrum. When utilizing a camera instead of single detectors, the differences in absorption due to an increased concentration of target gas are examined as a variation in pixel grayscale within the field of view of the camera. In the extreme case when the difference in radiant emittance is so great that the minimal detection limit of the camera is not met, the target gas will appear "blacked out" or as "black smoke" as outlined by work by the manufacturer [FLIR, 2005]. Real-time image visualizations of this nature are highly desired for a variety of applications in the defense, commercial and environmental communities. The quality and sensitivity of the detection engine relies heavily on the bandpass filter chosen for the target species of interest. Choice of the optimal filtering arrangement, both center wavelength and bandwidth must be reviewed for the entire range of target sensitivity to provide optimal detection performance. Prior to the high resolution radiance data of MODTRAN 5, optimization routines to better choose filter specifications were hampered by the lack of adequate resolution. However, with the 0.1 cm^{-1} resolution of MODTRAN 5™, we are able to simulate the integrated radiant emittance captured by a range of filtering configurations and examine the interferences. A result of this simulation applied to N_2O detection is shown by Figure 12.

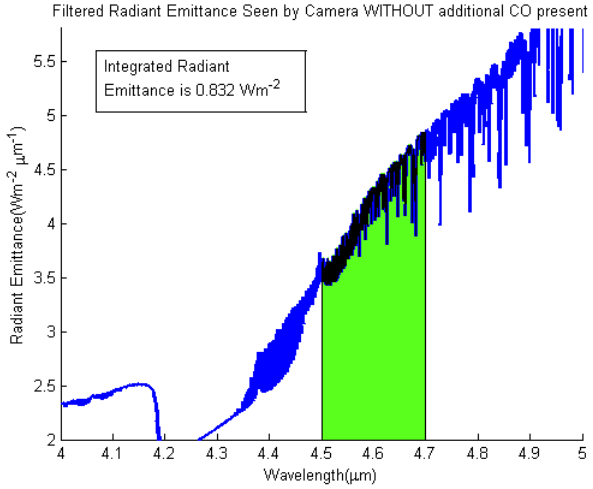

Figure 10. Filtered radiant emittance seen by sensor with background CO present.

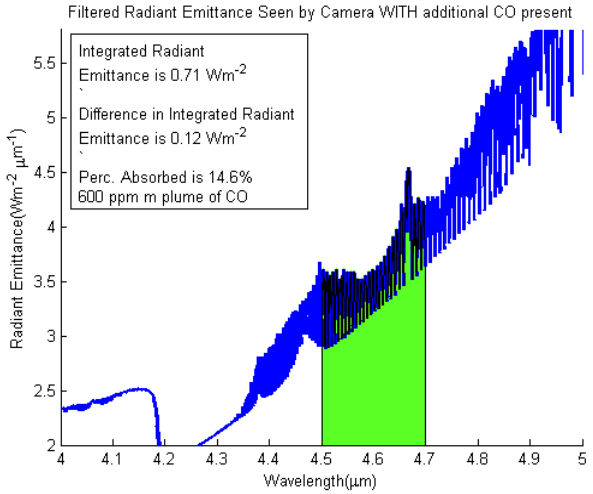

Figure 11. Filtered radiant emittance seen by sensor with additional CO present.

A MODTRAN 5™ simulation for the N_2O detection example using the radiance from a down-looking instrument is further explored. To extend our methodology to assist with selection of hardware, we plot the integrated radiance emittance as a function of filter bandwidth and center wavelength. In addition, we have included an approximate minimal detection limit parameter of 0.15 Wm^{-2} estimated for a commercially available MWIR camera [FLIR, 2005] operating in the given wavelength band of interest, see Figure 12. Without an increased target plume present in the far field, we must select a filter that allows the system to operate above

this limit, or the far field measurement will not be distinguishable. Quite simply, this leads to selection of a filter both in center wavelength (y-axis) and bandwidth (x-axis) to the right of the solid black line of detection limit.

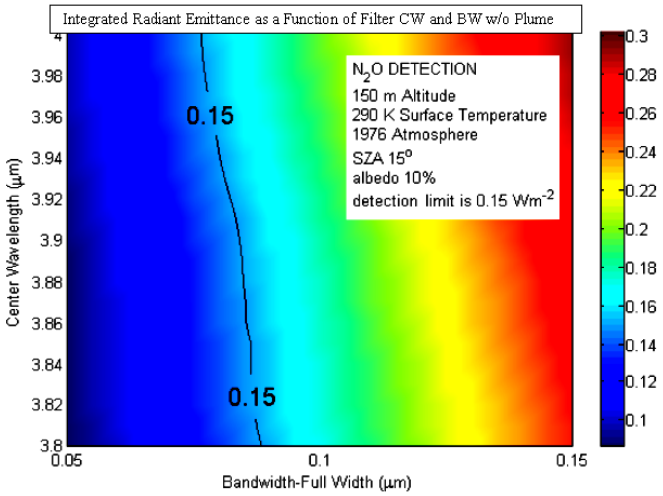

Figure 12. Simulated integrated radiant emittance captured by a range of filtering configurations, no plume present. (colorbar shows integrated radiant emittance, Wm^{-2})

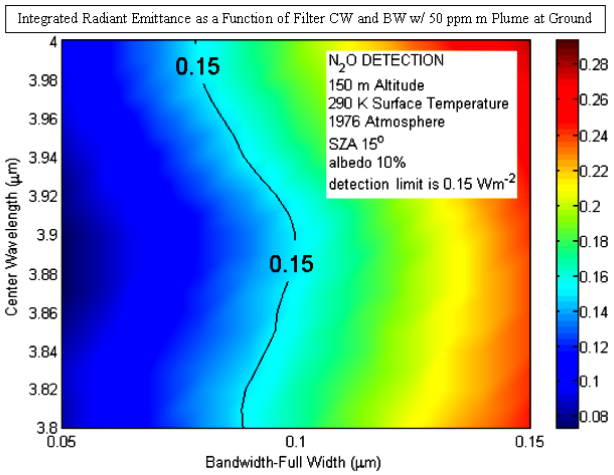

Figure 13. Simulated integrated radiant emittance captured by a range of filtering configurations, with 50 ppm·m plume present. (colorbar shows integrated radiant emittance, Wm^{-2})

As the target concentration is increased, the simulation can be re-run using the appropriate MODTRAN^{TM} 5 model and compared to the case of background atmospheric conditions. For this particular example, we review the previous example of a 50 ppm·m plume of N_2O at ground level (Figure 9, red line). Again, the detection limit is annotated in Figure 13 and the total integrated radiance is plotted as a function of bandwidth and center wavelength. Ideally, when a target is present, it is desirable to select conditions so that the location of the plume will appear darker than adjacent pixels in the field of view in the camera. A black plume will be observed for filter choices to the left of the detection limit indicated in Figure 13. When reviewing the model calculations of Figures 12 and 13, we conclude that for optimal performance of the detection mechanism for N_2O (right of limit in Figure 12, left of limit in Figure 13), the selected filter should have a bandwidth of 0.09 µm with a center wavelength of 3.9 µm. A further tradeoff to consider is the total percent difference in radiant emittance shown in Figure 14, and represents the total contrast. This plot follows from the same logic as the previous plots, but allows for the further optimization of the filter choice. The rule of thumb is to be above the detection limit for the atmospheric background case, and near the detection limit for the target species and concentration, while maximizing the total contrast.

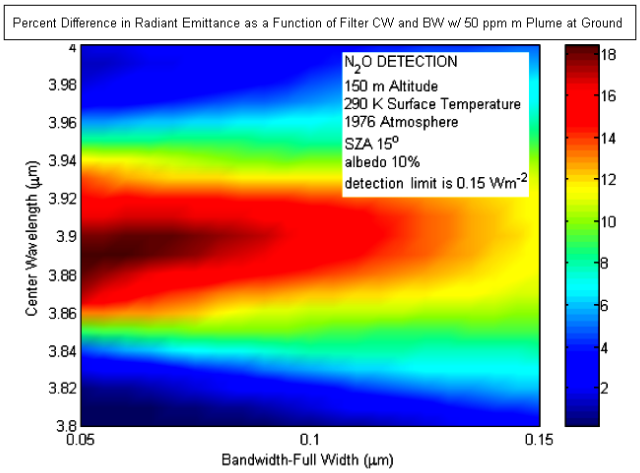

Figure 14. Contrast as described by the difference in radiant emittance for each center wavelength and filter bandwidth. Red areas indicate larger contrast more easily detectable regions of operation.

IV. Conclusion

High resolution of MODTRAN^{TM} 5 (0.1 cm^{-1} resolution) now makes it possible to resolve minor atmospheric constituents and simulate the atmospheric influence with realistic line widths. The capability is particularly important in the design of lidar and radiometric optical measurement systems. A white light differential analysis (DAS) and high resolution MODTRAN^{TM} 5 add-on has demonstrated methodology for measurement of trace species in the atmosphere. An initial example, which is the exploration of a specific water vapor band, is presented explicitly. By utilizing the mid-infrared spectrum (3 - 5 µm) along with MODTRAN^{TM} 5 it is possible to detect and quantify many trace constituents in the atmosphere, as indicated for the examples of nitrous oxide and carbon monoxide shown. These passive measurement techniques are applicable to many other trace constituents as well.

Acknowledgement

This paper was presented by Adam Willitsford at the AFRL Transmission Meeting for the 28th Review of Atmospheric Transmission Models 14-15 June 2006 at Lexington MA. The authors would like to thank Joe Begnoché (PSU) for his work

with the white light laser measurements. We would also like to thank ITT's remote sensing division (Steven V. Stearns, R. Todd Lines, Darryl G. Murdock, Matthew C. Severski, Dawn D. Lenz), and the PNNL data manager Steve Sharpe. Finally we appreciate the work of Gail Anderson, Jim Chetwynd and Michael Hoke and the host of contributors, past and present, who have worked on the development of MODTRAN™ 5.

REFERENCES

R. R. Alfano, *Supercontinuum Laser Source*, (Springer Verlag, New York), 1989.

A. Berk et al., "MODTRAN5: A reformulated atmospheric band model with auxiliary species and practical multiple scattering options," in Algorithms and Technologies for Multispectral, Hyperspectral, and Ultraspectral Imagery X, *Proceedings of SPIE*, v. 5425, S. Shen, ed., pp. 341 – 347, 2004.

J. Begnoché "Analytical Techniques for Laser Remote Sensing with a Supercontinuum White Light Laser" The Pennsylvania State University, M.S. Thesis, 2005.

FLIR Thermography. Boston, MA. www.flirthermography.com

T. Gosink "What Do Carbon Monoxide Levels Mean?" Alaska Science Forum Article #588, 1983
http://www.gi.alaska.edu/ScienceForum/ASF5/588.html

J.C. Knight, T.A. Birks, P.S. Russell and D.M. Atkin, "All-silica single-mode optical fiber with photonic crystal cladding," *Opt. Lett*. 21, 1547-1549, 1996

T. Lipman and M. Delucchi "Emissions of Nitrous Oxide and Methane from Conventional and Alternative Fuel Motor Vehicles" *Climatic Change* 53: 477-516, 2002.

C.R. Philbrick, Z. Liu, H. Hallen, D. Brown, A. Willitsford. "Lidar Techniques Applied To Remote Detection of Chemical Species in the Atmosphere, *Proceedings of the International Symposium on Spectral Sensing Research (ISSSR)*, 2006 (submitted).

J.K. Ranka, R.S. Windeler, and A.J. Stentz, "Visible continuum generation in air-silica microstructure optical fibers with anomalous dispersion at 800 nm," *Opt. Lett.* 25, 25-27, 2000.